



# OPEN The Impact of Russia-Ukraine geopolitical conflict on the air quality and toxicological properties of ambient PM<sub>2.5</sub> in Milan, Italy

Yashar Aghaei<sup>1</sup>, Mohammad Mahdi Badami<sup>1</sup>, Ramin Tohidi<sup>1</sup>, P. S. Ganesh Subramanian<sup>2</sup>, Roberto Boffi<sup>3</sup>, Alessandro Borgini<sup>3</sup>, Cinzia De Marco<sup>3</sup>, Paolo Contiero<sup>3</sup>, Ario Alberto Ruprecht<sup>3,4</sup>, Vishal Verma<sup>2</sup>, Talal Chatila<sup>5</sup> & Constantinos Sioutas<sup>1✉</sup>

The geopolitical conflict between Russia and Ukraine has disrupted Europe's natural gas supplies, driving up gas prices and leading to a shift towards biomass for residential heating during colder months. This study assessed the consequent air quality and toxicological impacts in Milan, Italy, focusing on fine particulate matter (PM<sub>2.5</sub>, d<sub>p</sub> < 2.5 μm) emissions. PM<sub>2.5</sub> samples were analyzed for their chemical composition and assessed for their oxidative potential using the dithiothreitol (DTT) assay across three periods reflecting residential heating deployment (RHD): pre-RHD, intra-RHD, and post-RHD periods. During the intra-RHD period, PM<sub>2.5</sub> levels were significantly higher than those in other periods, with concentrations reaching 57.94 ± 7.57 μg/m<sup>3</sup>, indicating a deterioration in air quality. Moreover, levoglucosan was 9.2 times higher during the intra-RHD period compared to the pre-RHD period, correlating with elevated levels of elemental carbon (EC) and polycyclic aromatic hydrocarbons (PAHs). These findings were compared with previous local studies before the conflict, underscoring a significant rise in biomass-related emissions. DTT assay levels during the intra-RHD were 2.1 times higher than those observed during the same period in 2022, strongly correlating with biomass burning emissions. Our findings highlight the necessity for policies to mitigate the indirect health effects of increased biomass burning emissions due to the energy crisis triggered by the geopolitical conflict.

The geopolitical tension between Russia and Ukraine has led to multifaceted effects in various sectors: while political relations and socio-economic aspects are at the forefront<sup>1</sup>, a critical implication demanding attention is the ensuing energy crisis, which poses significant risks to environmental and public health, including the potential exacerbation of air pollution levels<sup>2,3</sup>. Triggered by this energy crisis, the European Union (EU) has faced a substantial disruption in natural gas imports from Russia<sup>4,5</sup>, which escalated the prices of gas across European markets since early 2022<sup>6,7</sup>, leading to a roughly 20% decrease in natural gas consumption<sup>8</sup>. Although the EU has been extensively exploring alternative renewable energy sources with the aim of replacing natural gas<sup>9</sup>, biomass use for heat generation still stands as an economically viable alternative<sup>10</sup>. In line with this shift to biomass, the EU increased its imports by approximately 30% in 2022 compared to the preceding year<sup>8,11</sup>. As Italy has historically relied on both natural gas and biomass for residential energy demands, supported by previous studies on emissions and air quality<sup>12–14</sup>, it is positioned as an important case study for examining the levels and toxicity of atmospheric pollutants in the context of the current geopolitical conflict, which potentially shifts pollution sources.

Since the beginning of 2023, the Italian government has introduced tax reductions on wood pellets, a type of biomass, aimed to decrease residential heating costs and encourage the use of biomass for energy<sup>15</sup>. However, it is important to evaluate the impact of biomass burning on air quality, given that emissions from biomass combustion can contribute significantly to the levels of fine particulate matter (PM<sub>2.5</sub>, particle with aerodynamic

<sup>1</sup>Department of Civil and Environmental Engineering, University of Southern California, 3620 S. Vermont Ave. KAP210, Los Angeles, CA 90089, USA. <sup>2</sup>Department of Civil and Environmental Engineering, University of Illinois at Urbana Champaign, Urbana, IL, USA. <sup>3</sup>Fondazione IRCCS, Istituto Nazionale Tumori, Milan, Italy. <sup>4</sup>International Society of Doctors for Environment (ISDE), Arezzo, Italy. <sup>5</sup>Division of Immunology, Boston Children's Hospital, Harvard Medical School, Boston, MA, USA. ✉email: sioutas@usc.edu

diameter < 2.5  $\mu\text{m}$ ) in the air during the winter months<sup>16–18</sup>.  $\text{PM}_{2.5}$  can penetrate deep into the lungs and cause cardiovascular inflammation and lower the overall functions of the respiratory system<sup>19–21</sup>. The International Agency for Research on Cancer (IARC) classified ambient  $\text{PM}_{2.5}$  as a Group 1 carcinogen for lung cancer<sup>22,23</sup>, and epidemiological studies have also linked long-term exposure to these particles with an increased risk of lung cancer<sup>24–26</sup>. Although the total  $\text{PM}_{2.5}$  content of the ambient air has been linked to adverse impacts on human health<sup>27,28</sup>, specific chemical components, including carbonaceous species (i.e., organic carbon (OC), levoglucosan, and polycyclic aromatic hydrocarbons (PAHs)), have been consistently associated with the oxidative potential of  $\text{PM}_{2.5}$ <sup>29–31</sup>. Since these toxic components are major PM components of biomass burning emissions<sup>32–34</sup>, evaluation of their oxidative potential is essential for the investigation of the toxicity affecting residents subject to biomass activity emissions<sup>35–37</sup>.

Investigating the toxicity associated with these emissions is critical in areas prone to frequent air pollution episodes, such as the Po Valley in Italy's Lombardy region, which has experienced degraded air quality over the past few decades, particularly in the winter months<sup>38,39</sup>. One of the primary reasons for the persistent air quality issue is the geographical location of the valley, which is surrounded by the Alps and the Apennines mountains. This topographical situation, combined with stagnant meteorological conditions, limits the effective dispersion of air pollutants emitted in the valley<sup>40–42</sup>. Previous investigations indicated that during the warm seasons, the levels of ambient  $\text{PM}_{2.5}$  in the valley were mainly influenced by vehicular emissions and the formation of secondary organic aerosols<sup>43,44</sup>, while in the cold seasons, a combination of particular weather conditions and various emission sources, including biomass burning, can lead to severe air pollution episodes<sup>45,46</sup>. The ongoing energy crisis, driven by tensions between Russia and Ukraine, poses the risk of exacerbating the situation by possibly increasing the contribution of residential biomass burning as a source of pollution in the region. In addition to adverse impacts on air quality and public health, biomass burning contributes to climate change by emitting greenhouse gases and black carbon, influencing global warming through changes in solar radiative forces<sup>47,48</sup>.

This study aimed to determine potential changes in ambient  $\text{PM}_{2.5}$  chemical components impacting air quality and associated toxicity properties due to the geopolitical tensions between Russia and Ukraine. Ambient  $\text{PM}_{2.5}$  samples were collected within three distinct periods with consideration of the influence of residential heating deployment (RHD), including pre-RHD, intra-RHD, and post-RHD periods. The collected samples were analyzed for chemical species, and the dithiothreitol (DTT) assay was utilized to determine the oxidative potential of these samples. The levels of  $\text{PM}_{2.5}$  components and the associated toxicological characteristics were compared with previous investigations in that area conducted during winter before the conflict, enabling the observation of atmospheric pollutants' levels regardless of variations in meteorological factors from winter (i.e., intra-RHD) to other seasons (i.e., pre-RHD and post-RHD periods).

## Methods

### Sampling site and period

Sample collection was carried out at Bareggio, a Milan suburb area located 14 km northwest subjected to temperature variations, during three specific periods: pre-RHD period (late-October–early-November), intra-RHD period (late-November–February), and post-RHD period (mid-March–early-April) in 2022 and 2023. The region's rich historical air quality data<sup>12–14</sup>, long-standing history of biomass use for residential heating<sup>43,44</sup>, and unique topographical location<sup>40–42</sup>, alongside the energy policy changes<sup>15</sup>, driven by recent geopolitical tension between Russia and Ukraine, presented Milan as a prime case study for investigating the impacts of conflict on air quality. The meteorological conditions (i.e., temperature, relative humidity, and wind speed) within the sampling period were obtained from the closest meteorological station, the Roveda di Sedriano (MI) site in Bareggio, presented in Table S1. Low wind speed and relatively stable temperature further illustrated atmospheric conditions favoring pollutant accumulation, which were in agreement with previous studies documenting the Po Valley's stable atmospheric conditions, influencing air quality, especially in terms of  $\text{PM}_{2.5}$  concentration<sup>49,50</sup>.

A total of 17 ambient  $\text{PM}_{2.5}$  samples were collected on pre-baked quartz filters (37 mm, Pall Life Sciences, 2- $\mu\text{m}$  pore size, Ann Arbor, MI, USA) for weekly periods, utilizing two Sioutas Personal Cascade Impactor Samplers (PCISs, SKC Inc., Eighty-Four, PA, USA), each operating with a flow rate set at 9 L per minute<sup>51,52</sup>. The collected mass of  $\text{PM}_{2.5}$  was determined as the weight differential between the filters before and after sampling, following an equilibration process under controlled laboratory conditions, temperature range of 22–24 °C, and relative humidity range of 40–50%. This weight measurement was conducted using a microbalance (MT5, Mettler Toledo Inc., Columbus, OH, USA) with an accuracy level of  $\pm 0.001$  mg. Further details about the sampling procedure were provided in the supplementary information section.

### Chemical and toxicological analysis

The collected samples were subjected to chemical analysis at the Desert Research Institute (DRI) to determine their organic carbon (OC) and elemental carbon (EC) content, levoglucosan, polycyclic aromatic hydrocarbons (PAHs), water-soluble ions, as well as total metals. The measurement of OC and EC, as well as the assessment of the volatility of OC fractions, were conducted using a thermal/optical method<sup>53</sup>. Gas chromatography/mass spectrometry (GC/MS) was utilized to measure levoglucosan and other specific organic compounds<sup>54</sup>. Furthermore, ion chromatography (IC) and inductively coupled plasma mass spectrometry (ICP-MS) were employed to determine the concentrations of water-soluble inorganic ions as well as metals and trace elements<sup>55,56</sup>, respectively. The chemical components in the analysis included OC, EC, crustal metal and trace elements, and water-soluble inorganic ions (i.e.,  $\text{NH}_4^+$ ,  $\text{SO}_4^{3-}$ ,  $\text{NO}_3^-$ ,  $\text{PO}_4^{3-}$ ,  $\text{Cl}^-$ ,  $\text{Na}^+$ , and  $\text{K}^+$ ). To convert OC to organic matter (OM), we used a conversion factor of 2.0 for the intra-RHD period and 1.8 for the pre- and post-RHD periods<sup>57</sup>. For the evaluation of the oxidative potential, the DTT assay was employed by the Illinois Lab for Aerosol Research at the University of Illinois Urbana-Champaign, a widely used method for this purpose<sup>58–61</sup>. The oxidative potential

represents the capacity of PM to produce reactive oxygen species that can lead to oxidative stress, potentially resulting in adverse health outcomes<sup>62</sup>. In the DTT assay, the consumption rate of DTT reflects the oxidative potential of the PM samples, as it measures the decline in cellular antioxidants due to their conversion to their disulfide states<sup>63</sup>. Previous studies have identified various PM constituents, including PAHs and metals like Fe, Cu, Ni, Mn, and Zn, as contributing factors to the rate of DTT depletion<sup>64,65</sup>. In this study, collected samples on quartz filter extracted in methanol were filtered in a cell-free system, and the linear rate of DTT depletion was determined per time unit. Further details about the operation of the DTT assay are available in earlier literature<sup>62,66</sup>. The rate of DTT consumption was normalized to the volume of the air sampled, obtaining intrinsic oxidative potentials measured in the unit of nmol/(min m<sup>3</sup>). Further details about chemical and toxicological analyses, as well as quality assurance and control, were provided in the supplementary information section.

## Results and discussion

### Total mass concentrations

Figure 1 shows the mass concentrations of the collected PM<sub>2.5</sub> in samples with contributed chemical components and average ambient temperatures during measurement periods to observe the influence of domestic heating deployment.

As shown in Fig. 1, the concentration of PM<sub>2.5</sub> was significantly higher during the intra-RHD period, averaging  $57.94 \pm 7.57 \mu\text{g}/\text{m}^3$ , compared to  $22.61 \pm 1.64$  and  $23.13 \pm 2.27 \mu\text{g}/\text{m}^3$  in the pre- and post-RHD periods. A significant increase in the mass concentration of total PM<sub>2.5</sub> was observed during the intra-RHD period for a range of constituents, including OM, EC, crustal metals and trace elements, and water-soluble ions (i.e., NH<sub>4</sub><sup>+</sup> SO<sub>4</sub><sup>2-</sup>, NO<sub>3</sub><sup>-</sup>, PO<sub>4</sub><sup>3-</sup>, Cl<sup>-</sup>, Na<sup>+</sup>, and K<sup>+</sup>) with recorded values as 16.56, 5.50, 6.32, and 16.46  $\mu\text{g}/\text{m}^3$ , respectively. However, average PM<sub>2.5</sub> mass concentrations during wintertime in 2020 were reported to be  $42.63 \pm 16.47 \mu\text{g}/\text{m}^3$ , which was lower than our reported PM<sub>2.5</sub> concentration. While lower temperatures and restricted atmospheric mixing height contribute to elevated pollutant levels<sup>49,50</sup>, the significant difference in PM<sub>2.5</sub> concentration between the cold months of 2023 and 2020 shows an exacerbating air quality condition, likely due to changes in emission sources contributing to the elevated PM<sub>2.5</sub> levels, which will be explored in the following sections through the analysis of PM<sub>2.5</sub> chemical components.

### Trace elements and metals

The average concentrations of trace elements and transition metals during the pre-, intra-, and post-RHD periods in our sampling location are presented in Fig. 2. The chemical speciation commonly associated with industrial emissions (e.g., Se, As, Cd, Pb, and V)<sup>68-70</sup>, as well as mineral and road dust emissions (e.g., Fe, Li, Cr, Mn, Ni, Cu, Zn, and Ba)<sup>71-73</sup>, showed higher levels during the intra-RHD period, which were approximately between 1.5 and 1.7 times higher than pre- and post-RHD periods. In the Po Valley, the majority of PM<sub>2.5</sub>-bound metals and trace elements primarily originate from anthropogenic sources (e.g., vehicle emissions and industrial operations)<sup>43,44,74</sup>, which have relatively stable emissions throughout the year<sup>46</sup>, so the temporal variations of these emitted species are influenced mainly by seasonal weather conditions<sup>42,50</sup>.

The mass concentration of K, a biomass burning chemical marker<sup>75</sup>, increased during the intra-RHD period to 771.86 ng/m<sup>3</sup>, with concentrations of 4.5 and 3.8 times higher than the pre- and post-RHD periods. This significant rise in K mass concentration cannot be solely explained by meteorological conditions. The increased K values were potentially attributed to elevated biomass burning emissions within the intra-RHD period when

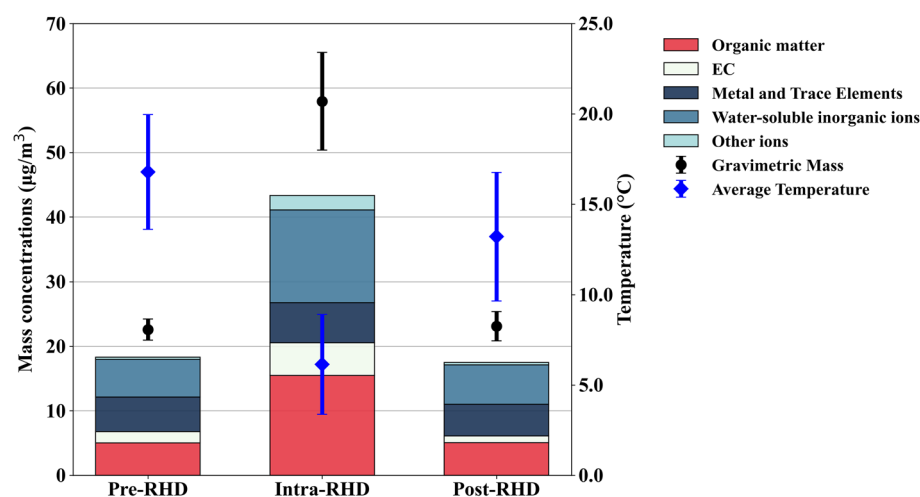


**Figure 1.** Mass concentrations of the collected PM<sub>2.5</sub> samples with their chemical composition and average temperature across different measurement periods (i.e., pre-, intra-, and post-RHD). Error bars on the graphs represent the standard deviation, indicating the variability for average temperature and gravimetric mass of the PM<sub>2.5</sub> samples.

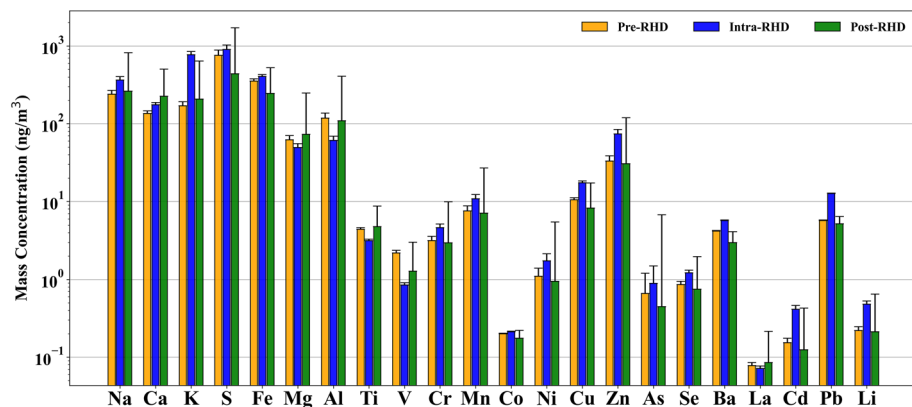


**Figure 2.** Average concentrations of trace elements and transition metals across different measurement periods (i.e., pre-, intra-, and post-RHD). Error bars on the graphs represent the Standard deviation, indicating the variability for the concentration of each element in the PM<sub>2.5</sub> samples.

people switched from using natural gas to biomass for residential heating purposes, which could be justified by the significant difference between the ratio of the intra-RHD period to the other periods.

### Carbonaceous components

Figure 3 displays the average concentrations of carbonaceous components over the pre-, intra-, and post-RHD periods. Both OC and EC displayed higher mass concentrations during the intra-RHD period, with values reported as 8.28 and 5.50 µg/m<sup>3</sup>, respectively. The OC concentration during the intra-RHD period was approximately 2.9 times higher than those observed during both the pre- and post-RHD periods. Similarly, the EC level increased, reaching 3.2 times higher compared to the pre-RHD period and 5.3 times higher than the post-RHD period (see Fig. 3a).

Levoglucosan, which has been used as a tracer of biomass burning<sup>76</sup>, exhibited increased value during the intra-RHD period, with a concentration of 1335.0 ng/m<sup>3</sup>. The levoglucosan level during the intra-RHD period was 7.7 times higher than those observed during the pre-RHD period and 9.2 times higher than the post-RHD period.

PAHs are carbonaceous components consisting of multiple aromatic rings produced during the incomplete combustion of fossil fuels and biomass burning<sup>77,78</sup>. During the intra-RHD period, the PAHs levels showed a similar pattern, with an increased concentration of 45.18 ng/m<sup>3</sup>, which was 14.5 and 17.5 times higher than the pre- and post-RHD periods, respectively. Among individual PAHs, chrysene, pyrene, benzo[a]pyrene, and benzo[ghi]perylene are found to be particularly abundant in biomass burning emissions<sup>45,79</sup>, which showed higher levels during the intra-RHD period compared to the two other periods. Chrysene and pyrene showed an approximate 25 and ninefold increase from 0.31 and 0.41 ng/m<sup>3</sup> in the pre-RHD to 7.98 and 3.74 ng/m<sup>3</sup> during the intra-RHD period, respectively, and these values decreased to 0.35 and 0.38 ng/m<sup>3</sup> in the post-RHD period. Similarly, benzo[a]pyrene and benzo[ghi]perylene showed higher concentrations during the intra-RHD period, with values reported as 5.26 and 7.36 ng/m<sup>3</sup>, respectively, which are 22 and 12 times higher than those recorded during the pre-RHD period; subsequently, these values declined to 0.17 and 0.42 ng/m<sup>3</sup> in the post-RHD period.

Although increased levels of the carbonaceous species can be partially attributed to more stable atmospheric wintertime conditions<sup>50,80</sup>, which limit effective dispersion in the atmosphere<sup>46,81</sup>, this alone cannot fully account for the observed high concentrations. During the intra-RHD period, the elevated concentrations of biomass burning tracers, including levoglucosan and PAHs, along with the strong linear correlations observed between levoglucosan and total PAHs ( $R^2 = 0.95$ ,  $p$ -value < 0.001), as well as EC ( $R^2 = 0.97$ ,  $p$ -value < 0.001), demonstrate the significant impact of biomass burning on the rise in carbonaceous component levels.

A comparison of our reported carbonaceous species concentrations with earlier studies in this region during cold months is presented in Table 1. In our study, the concentration of PM<sub>2.5</sub>-bound OC, a marker for both traffic and biomass burning emissions, was in a comparable range with PM<sub>10</sub>-bound OC measurements from several locations across the Po Valley<sup>16,67</sup>. Additionally, the OC levels reported in our study were higher than those in other studies focusing on ambient PM<sub>2.5</sub><sup>43,44,82</sup>. Similarly, the EC level measured during the intra-RHD period was higher than previously recorded values across the region for the same time span in past years, highlighting the effect of increased domestic biomass burning during the ongoing conflict. The levoglucosan mass concentration observed in our study was significantly higher than the previously reported values at urban/rural locations in Po Valley<sup>16,43,44,67,82</sup>. The concentrations of PAHs measured during the intra-RHD period were also notably higher than those in urban and suburban regions of Milan<sup>16,43,44,67,82</sup>, and even exceeded levels found on sites in Beijing, Wuhan, and Shanghai with the average value of 34.37 ng/m<sup>3</sup><sup>83</sup>. Moreover, the PAHs levels in our study were comparable to those in polluted urban/suburban areas in the Czech Republic, with an average of 39.25 ng/m<sup>3</sup><sup>84</sup>. Additionally, Table 1 shows a comparison between three distinct periods: normal life and traffic patterns in 2020 (January–February), the first lockdown period of COVID-19 in 2020 (March), and our study during the intra-RHD period in 2023, affected by the ongoing conflict. There was a noticeable decrease in the levels of

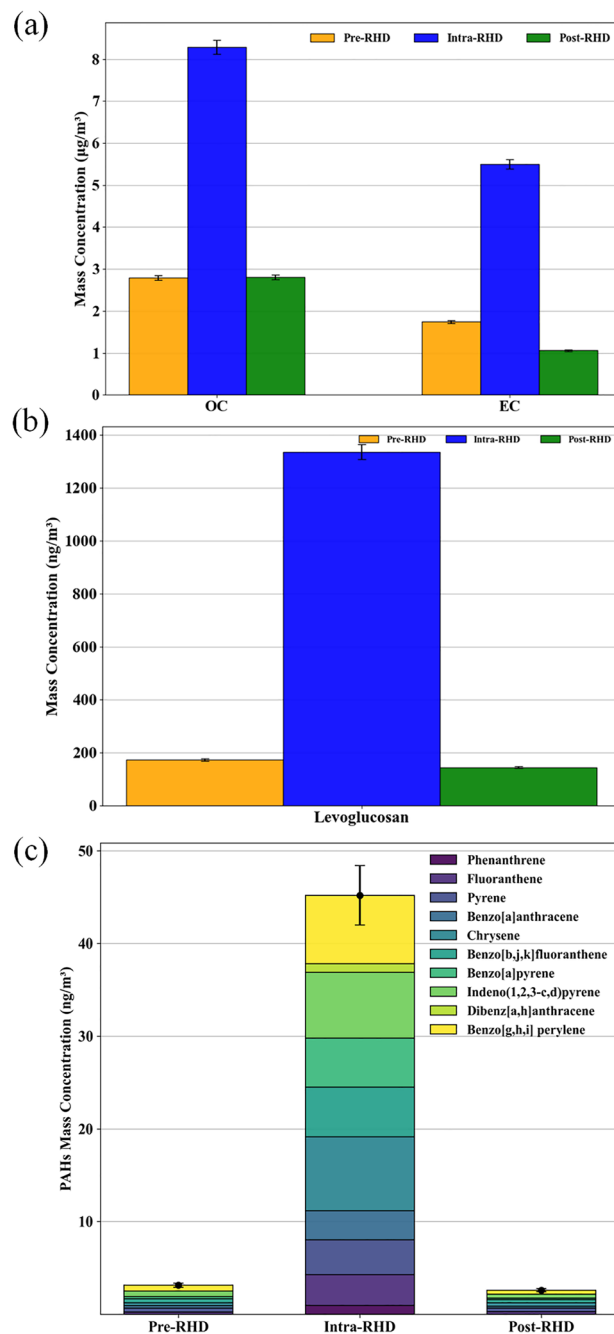


**Figure 3.** Average concentrations of (a) OC and EC, (b) levoglucosan, and (c) individual PAH species across different measurement periods (i.e., pre-, intra-, and post-RHD). Error bars on the graphs represent the standard deviation, indicating the variability for the concentration of each component in the PM<sub>2.5</sub> samples.

carbonaceous components during the pandemic<sup>82</sup> compared to the pre-pandemic period<sup>16</sup>, a reduction that is likely attributable to decreased human activity and traffic at that time. Our findings showed higher levels of EC, levoglucosan, and PAHs during the intra-RHD period compared to those reported during the pre-pandemic by Pietrogrande et al.<sup>16</sup>. Considering that EC can also be a tracer of traffic emissions, we conducted further analysis to determine whether traffic might be contributing to its increased levels. Table 2 displays data from the Environmental Protection Agency of Lombardy (Agenzia Regionale per la Protezione Ambientale (ARPA)) website for Milan—via Pascal air quality station on specific markers for traffic emissions (i.e., NO<sub>2</sub> and C<sub>6</sub>H<sub>6</sub>)<sup>85–87</sup> and contrasts these levels during the measurement periods of our study and the study conducted by Pietrogrande et al.<sup>16</sup>.

Both NO<sub>2</sub> and C<sub>6</sub>H<sub>6</sub> levels were slightly lower in 2023 compared to the same timeframe in 2020 (*p*-value < 0.05), suggesting a small decrease in traffic-related emissions in 2023. As a result, the high levels of EC observed in our study suggest an alternative emission source rather than traffic emissions significantly contributes to atmospheric

Study	Year	Sample	Species			
			OC ( $\mu\text{g}/\text{m}^3$ )	EC ( $\mu\text{g}/\text{m}^3$ )	PAHs ( $\text{ng}/\text{m}^3$ )	Levoglucosan ( $\text{ng}/\text{m}^3$ )
Current study	2023	PM <sub>2.5</sub>	8.28 ± 0.16	5.50 ± 0.11	45.18 ± 3.27	1335.0 ± 28.25
Perrone et al. <sup>44</sup>	2006–09	PM <sub>2.5</sub>	6.04	–	25.8 ± 4.3	502 ± 134
Altuwayjiri et al. <sup>82</sup>	2020	PM <sub>2.5</sub>	2.41 ± 0.14	0.28 ± 0.03	1.42 ± 0.21	53.85 ± 8.06
Daher et al. <sup>43</sup>	2009–10	PM <sub>10</sub>	11.65	0.75	7.47	53
Pietrogrande et al. <sup>16</sup>	2020	PM <sub>10</sub>	10.38 ± 4.23	1.64 ± 0.9	3.71 ± 3.77	1100 ± 710
Pietrogrande et al. <sup>67</sup>	2020	PM <sub>10</sub>	11.10 ± 4.56	1.47 ± 0.83	2.82 ± 2.22	1070 ± 720

**Table 1.** Comparison of biomass burning tracers during the winter months in the region.

Month/year	NO <sub>2</sub> ( $\mu\text{g}/\text{m}^3$ )		C <sub>6</sub> H <sub>6</sub> ( $\mu\text{g}/\text{m}^3$ )	
	2023	2020	2023	2020
January	40.74	56.07	2.49	3.8
February	40.47	44.83	1.96	2.01

**Table 2.** Comparison of traffic-related emissions during the winter months.

pollutants. Given that traffic emissions during our 2023 measurement period were comparable to pre-pandemic levels in 2020, the rise in the levels of carbonaceous compounds in our study aligns with Italy's tax reduction for biomass, suggesting these policies have boosted biomass burning for residential heating.

### Oxidative potential of PM<sub>2.5</sub>

Previous research conducted in the Po Valley indicated that the oxidative potential of PM is mainly driven by certain metals (e.g., Cr, Mn, Fe, Ni, and Cu), as well as carbonaceous compounds such as OC, levoglucosan, and PAHs<sup>59,88,89</sup>. Figure 4 shows the results of PM<sub>2.5</sub> oxidative potential as measured by the DTT assay of collected samples. During the intra-RHD period in 2023, with the significant increase of biomass burning tracers in PM<sub>2.5</sub> composition (i.e., levoglucosan and PAHs), the oxidative potential measured by DTT assay showed an elevated level of 1.64 nmol/(min m<sup>3</sup>), which was 3.6 times higher than those observed during the post-RHD in 2023. To further analyze the toxicity of PM<sub>2.5</sub> emissions, the oxidative potential of collected samples during the intra-RHD period in the preceding year was evaluated. During the intra-RHD period in 2022, DTT analysis showed a higher value of 0.78 nmol/(min m<sup>3</sup>), which was 2.6 times higher than those observed during the post-RHD in 2022, which is in line with the trend we observed in 2023. One factor that could increase the oxidative potential is stable atmospheric conditions prevailing in the winter, leading to the accumulation and aging of particles in the atmosphere<sup>42,44,90</sup>, thereby amplifying their oxidative potential and, consequently, their toxicity. However, for the intra-RHD periods, the DTT activity in 2023 was 2.1 times higher than the levels observed in 2022, indicating increased oxidative potential in PM<sub>2.5</sub> samples. For the post-RHD periods, the DTT findings were comparable in both years, with observed values of 0.45 and 0.29 nmol/(min m<sup>3</sup>) in 2023 and 2022, respectively. While the measured DTT analysis during the post-RHD was consistent with findings in both years, the result

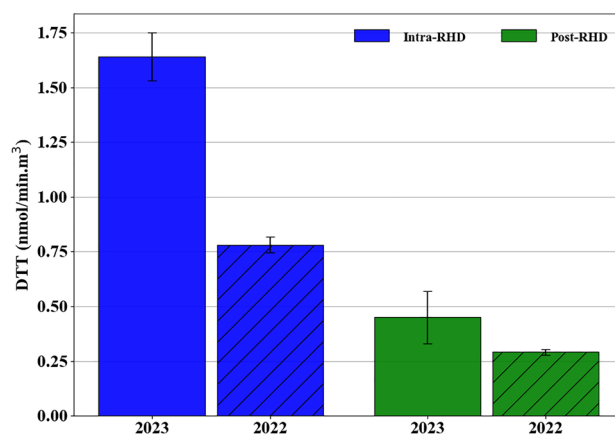


**Figure 4.** PM<sub>2.5</sub> oxidative potential as measured by the DTT assay across intra- and post-RHD periods in 2022 and 2023. Error bars on the graphs represent the standard deviation, indicating the variability for the DTT assay in the PM<sub>2.5</sub> samples.

during the intra-RHD period in 2023 was notably higher in contrast to the previous year, suggesting that the high-density emissions from biomass burning could be another key factor in increasing the oxidative potential of ambient PM<sub>2.5</sub>.

In Table 3, we compared levels of DTT activity in the current study to data from earlier studies in the same area during the winter before the geopolitical tensions. The oxidative potential measured by the DTT assay reported in 2023 was significantly higher than both our measurements in 2022 and previous investigations<sup>16,82,91</sup>. Despite a slight reduction in road traffic, the findings indicated that the PM<sub>2.5</sub> toxicity in the urban background site of the Bareggio is drastically increased compared to previous investigations in the region, suggesting that biomass combustion emissions rather than road traffic are possibly contributing significantly to elevated oxidative potential. These observations align with increased mass concentrations of the collected PM<sub>2.5</sub> and raised concentrations of biomass combustion markers in the intra-RHD period, as covered in previous sections.

To better understand the influence of residential biomass burning emissions on the oxidative potential of PM<sub>2.5</sub>, we conducted a statistical analysis to determine the correlation between DTT activity and the mass concentrations of specific chemical PM<sub>2.5</sub> compounds. Table 4 presents the findings from a Spearman rank regression analysis, which explored the relationship between DTT activity and the chemical compounds. Our analysis showed strong correlations between DTT activity levels and carbonaceous compounds, such as EC, levoglucosan, and PAHs (*p*-values < 0.05), highlighting the importance of biomass burning tracers in the oxidative potential and toxicity of PM<sub>2.5</sub> particles. While biomass combustion markers were highly correlated with the DTT activity, trace elements (e.g., Se, Pb, V, Fe, Li, Cr, Mn, Ni, Cu, Zn, and Ba) and water-soluble inorganic ions (e.g., NH<sub>4</sub><sup>+</sup>, SO<sub>4</sub><sup>3-</sup>, NO<sub>3</sub><sup>-</sup>) showed relatively weak correlations. The strong correlation between biomass burning tracers and the oxidative potential of PM<sub>2.5</sub> further corroborates the major role of biomass burning in the adverse indirect health impacts. It should be noted that epidemiological studies have linked exposure to PM<sub>2.5</sub>-bound OC and EC to increased cardiovascular disease admissions, heightened inflammatory responses, blood pressure changes, and respiratory inflammation<sup>92–95</sup>. PAH was also associated with increased inflammatory markers such as interleukin-6, indicating potential respiratory and systemic inflammation<sup>96</sup>, highlighting the significant health risks posed by geopolitical tensions between Russia and Ukraine.

## Conclusions

This study aimed to assess the concentrations of ambient PM<sub>2.5</sub> and its constituents, as well as the oxidative potential in Milan, Italy, in response to the geopolitical tensions between Russia and Ukraine, which likely prompted a shift to biomass-based residential heating during colder months. To evaluate the effects of this change in heating sources on air pollution, PM<sub>2.5</sub> samples were collected in the suburban region of Milan using two PCISs during cold and warm periods to consider the effect of residential heating deployment: pre-, intra-, and post-RHD periods. Our findings indicated a substantial rise in PM<sub>2.5</sub> levels and biomass burning markers, such as K, levoglucosan, PAHs, and EC, during the intra-RHD period, which were among the highest levels reported

Study	Year	Samples	DTT nmol/(min m <sup>3</sup> )
Current study	2023	PM <sub>2.5</sub>	1.64 ± 0.11
Current study	2022	PM <sub>2.5</sub>	0.78 ± 0.03
Altuwayjiri et al. <sup>82</sup>	2020	PM <sub>2.5</sub>	0.73 ± 0.13
Simonetti et al. <sup>91</sup>	2017	PM <sub>10</sub>	0.07 ± 0.01
Pietrogrande et al. <sup>16</sup>	2020	PM <sub>10</sub>	0.62 ± 0.15
Pietrogrande et al. <sup>67</sup>	2020	PM <sub>10</sub>	0.39 ± 0.15

**Table 3.** Comparison of DTT activity during the winter months in the region.

Species	DTT activity		Species	DTT activity	
	R	P-value		R	P-value
PAHs	<b>0.88</b>	<b>0.01</b>	Li	0.14	0.78
Levoglucosan	<b>0.77</b>	<b>0.05</b>	Cr	0.42	0.39
EC	<b>0.82</b>	<b>0.03</b>	Mn	0.20	0.70
OC	<b>0.71</b>	<b>0.10</b>	Ni	0.42	0.39
K	<b>0.94</b>	<b>0.004</b>	Cu	0.48	0.32
As	<b>0.82</b>	<b>0.03</b>	Zn	0.25	0.62
Cd	<b>0.77</b>	<b>0.05</b>	Ba	0.60	0.20
Pb	0.60	0.20	NH <sub>4</sub> <sup>+</sup>	-0.31	0.54
V	-0.65	0.15	SO <sub>4</sub> <sup>2-</sup>	-0.37	0.46
Fe	0.20	0.70	NO <sub>3</sub> <sup>-</sup>	0.25	0.62

**Table 4.** Spearman correlation coefficients between the DTT activity (nmol/(min m<sup>3</sup>) air) and mass concentration (µg/m<sup>3</sup>) of different chemical species. Values in Bold indicate statistically significant correlations.

in prior studies conducted regionally. Of particular note, the PM<sub>2.5</sub> oxidative potential increased up to 2 times during the intra-RHD period, as opposed to the levels reported in recent studies in the area. Our statistical analysis showed that biomass burning tracers had significant correlations with elevated DTT activity, indicating potential health hazards associated with changes in heating practices due to energy considerations. Furthermore, our study highlights the considerable impact of biomass combustion markers on PM<sub>2.5</sub> concentration and toxicity within Milan's metropolitan area, necessitating policy action to mitigate these emissions and their harmful indirect health effects. Research into cleaner biomass technologies, combined with policy incentives for renewable energy adoption such as wind power, alongside the updating of building standards for higher energy efficiency, can significantly contribute to improvements in air quality and public health.

## Data availability

All data used in this paper are available from the authors upon request.

Received: 22 November 2023; Accepted: 22 February 2024

Published online: 12 March 2024

## References

1. Khudaykulova, M., Yuanqiong, H. & Khudaykulov, A. Economic Consequences and Implications of the Ukraine-Russia War. *Int. J. Manag. Sci. Bus. Admin.* **8**, 44–52 (2022).
2. Borowski, P. F. Mitigating climate change and the development of green energy versus a return to fossil fuels due to the energy crisis in 2022. *Energies* **15**, 9289 (2022).
3. Pereira, P., Bašić, F., Bogunovic, I. & Barcelo, D. Russian-Ukrainian war impacts the total environment. *Sci. Total Environ.* **837**, 155865 (2022).
4. Kuzemko, C., Blondeel, M., Dupont, C. & Brisbois, M. C. Russia's war on Ukraine, European energy policy responses & implications for sustainable transformations. *Energy Res. Soc. Sci.* **93**, 102842 (2022).
5. Russia's War on Ukraine – Topics - IEA. <https://www.iea.org/topics/russias-war-on-ukraine>.
6. Mbah, R. E. & Wasum, D. F. Russian-Ukraine 2022 War: A review of the economic impact of Russian-Ukraine crisis on the USA, UK, Canada and Europe. *Adv. Soc. Sci. Res. J.* **9**, 144–153 (2022).
7. Liadze, I., Macchiarelli, C., Mortimer-Lee, P. & Sanchez Juanino, P. Economic costs of the Russia-Ukraine war. *World Econ.* **46**, 874–886 (2023).
8. Database - Eurostat. <https://ec.europa.eu/eurostat/web/main/data/database>.
9. Europe – Countries & Regions - IEA. <https://www.iea.org/regions/europe>.
10. Popp, J., Kovács, S., Oláh, J., Divéki, Z. & Balázs, E. Bioeconomy: Biomass and biomass-based energy supply and demand. *N. Biotechnol.* **60**, 76–84 (2021).
11. Home | Global Agricultural Information Network. <https://gain.fas.usda.gov/#/home>.
12. Daellenbach, K. R. *et al.* Organic aerosol sources in the Milan metropolitan area – Receptor modelling based on field observations and air quality modelling. *Atmos. Environ.* **307**, 119799 (2023).
13. Brege, M. *et al.* Molecular insights on aging and aqueous-phase processing from ambient biomass burning emissions-influenced Po Valley fog and aerosol. *Atmos. Chem. Phys.* **18**, 13197–13214 (2018).
14. Ricciardelli, I. *et al.* A three-year investigation of daily PM<sub>2.5</sub> main chemical components in four sites: The routine measurement program of the Supersito Project (Po Valley, Italy). *Atmos. Environ.* **152**, 418–430 (2017).
15. Ministero dell'Economia e delle Finanze - Home Page. <https://www.mef.gov.it/>.
16. Pietrogrande, M. C., Demaria, G., Colombi, C., Cuccia, E. & Dal Santo, U. Seasonal and Spatial Variations of PM<sub>10</sub> and PM<sub>2.5</sub> Oxidative Potential in Five Urban and Rural Sites across Lombardia Region, Italy. *Int. J. Environ. Res. Public Health* **19**, 7778 (2022).
17. Lonati, G., Giugliano, M. & Ozgen, S. Primary and secondary components of PM<sub>2.5</sub> in Milan (Italy). *Environ. Int.* **34**, 665–670 (2008).
18. Sirignano, C. *et al.* High contribution of biomass combustion to PM<sub>2.5</sub> in the City Centre of Naples (Italy). *Atmosphere* **10**, 451 (2019).
19. Willers, S. M. *et al.* Fine and coarse particulate air pollution in relation to respiratory health in Sweden. *Eur. Respir. J.* **42**, 924–934 (2013).
20. Xing, Y. F., Xu, Y. H., Shi, M. H. & Lian, Y. X. The impact of PM<sub>2.5</sub> on the human respiratory system. *J. Thorac. Dis.* **8**, E69–E74 (2016).
21. Valavanidis, A., Fiotakis, K. & Vlachogianni, T. Airborne particulate matter and human health: Toxicological assessment and importance of size and composition of particles for oxidative damage and carcinogenic mechanisms. *J. Environ. Sci. Health C Environ. Carcinog. Ecotoxicol. Rev.* **26**, 339–362 (2008).
22. Loomis, D. *et al.* The carcinogenicity of outdoor air pollution. *Lancet Oncol.* **14**, 1262–1263 (2013).
23. Volume 109: Outdoor Air Pollution – IARC Monographs on the Identification of Carcinogenic Hazards to Humans. <https://monographs.iarc.who.int/news-events/volume-109-outdoor-air-pollution/> (2013).
24. Raaschou-Nielsen, O. *et al.* Air pollution and lung cancer incidence in 17 European cohorts: Prospective analyses from the European Study of Cohorts for Air Pollution Effects (ESCAPE). *Lancet Oncol.* **14**, 813–822 (2013).
25. Gharibvand, L. *et al.* The association between ambient fine particulate air pollution and lung cancer incidence: Results from the AHSMOG-2 study. *Environ. Health Perspect.* **125**, 378–384 (2017).
26. Hvidtfeldt, U. A. *et al.* Long-term low-level ambient air pollution exposure and risk of lung cancer – A pooled analysis of 7 European cohorts. *Environ. Int.* **146**, 106249 (2021).
27. Boldo, E. *et al.* Health impact assessment of a reduction in ambient PM<sub>2.5</sub> levels in Spain. *Environ. Int.* **37**, 342–348 (2011).
28. Lu, F. *et al.* Systematic review and meta-analysis of the adverse health effects of ambient PM<sub>2.5</sub> and PM<sub>10</sub> pollution in the Chinese population. *Environ. Res.* **136**, 196–204 (2015).
29. Jedynska, A. Spatial variations and development of land use regression models of PAH, EC/OC, levoglucosan and oxidative potential of PM<sub>2.5</sub> in European study areas. (2016).
30. Pirhadi, M., Mousavi, A., Taghvaei, S., Shafer, M. M. & Sioutas, C. Semi-volatile components of PM<sub>2.5</sub> in an urban environment: Volatility profiles and associated oxidative potential. *Atmos. Environ.* **223**, 117197 (2020).
31. Akhtar, U. S. *et al.* Cytotoxic and proinflammatory effects of ambient and source-related particulate matter (PM) in relation to the production of reactive oxygen species (ROS) and cytokine adsorption by particles. *Inhal. Toxicol.* **22**, 37–47 (2010).
32. Li, W. *et al.* Tracers from biomass burning emissions and identification of biomass burning. *Atmosphere* **12**, 1401 (2021).
33. de Oliveira Alves, N. *et al.* Biomass burning in the Amazon region: Aerosol source apportionment and associated health risk assessment. *Atmos. Environ.* **120**, 277–285 (2015).

34. Saarikoski, S. *et al.* Chemical characterization of springtime submicrometer aerosol in Po Valley Italy. *Atmos. Chem. Phys.* **12**, 8401–8421 (2012).
35. Kelly, F. J. & Fussell, J. C. Global nature of airborne particle toxicity and health effects: A focus on megacities, wildfires, dust storms and residential biomass burning. *Toxicol. Res. (Camb)* **9**, 331–345 (2020).
36. Samburova, V. *et al.* Polycyclic aromatic hydrocarbons in biomass-burning emissions and their contribution to light absorption and aerosol toxicity. *Sci. Total Environ.* **568**, 391–401 (2016).
37. Sarigiannis, D. A., Karakitsios, S. P., Zikopoulos, D., Nikolaki, S. & Kermenidou, M. Lung cancer risk from PAHs emitted from biomass combustion. *Environ. Res.* **137**, 147–156 (2015).
38. Conticini, E., Frediani, B. & Caro, D. Can atmospheric pollution be considered a co-factor in extremely high level of SARS-CoV-2 lethality in Northern Italy?. *Environ. Pollut.* **261**, 114465 (2020).
39. Putaud, J. P., Van Dingenen, R. & Raes, F. Submicron aerosol mass balance at urban and semirural sites in the Milan area (Italy). *J. Geophys. Res. Atmos.* **107**, LOP-11 (2002).
40. Caserini, S., Giani, P., Cacciamani, C., Ozgen, S. & Lonati, G. Influence of climate change on the frequency of daytime temperature inversions and stagnation events in the Po Valley: Historical trend and future projections. *Atmos. Res.* **184**, 15–23 (2017).
41. Pernigotti, D., Georgieva, E., Thunis, P. & Bessagnet, B. Impact of meteorology on air quality modeling over the Po valley in northern Italy. *Atmos. Environ.* **51**, 303–310 (2012).
42. Tositti, L. *et al.* Source apportionment of particulate matter in a large city of southeastern Po Valley (Bologna, Italy). *Environ. Sci. Pollut. Res.* **21**, 872–890 (2014).
43. Daher, N. *et al.* Characterization, sources and redox activity of fine and coarse particulate matter in Milan Italy. *Atmos. Environ.* **49**, 130–141 (2012).
44. Perrone, M. G. *et al.* Sources of high PM<sub>2.5</sub> concentrations in Milan Northern Italy: Molecular marker data and CMB modelling. *Sci. Total Environ.* **414**, 343–355 (2012).
45. Belis, C. A. *et al.* Sources for PM air pollution in the Po Plain, Italy: I. Critical comparison of methods for estimating biomass burning contributions to benzo(a)pyrene. *Atmos. Environ.* **45**, 7266–7275 (2011).
46. Vecchi, R., Marazzan, G., Valli, G., Ceriani, M. & Antoniazzi, C. The role of atmospheric dispersion in the seasonal variation of PM1 and PM<sub>2.5</sub> concentration and composition in the urban area of Milan (Italy). *Atmos. Environ.* **38**, 4437–4446 (2004).
47. Ramanathan, V. & Carmichael, G. Global and regional climate changes due to black carbon. *Nat. Geosci.* **1**, 221–227 (2008).
48. Boucher, O. & Reddy, M. S. Climate trade-off between black carbon and carbon dioxide emissions. *Energy Policy* **36**, 193–200 (2008).
49. Marazzan, G. M., Vaccaro, S., Valli, G. & Vecchi, R. Characterisation of PM10 and PM<sub>2.5</sub> particulate matter in the ambient air of Milan (Italy). *Atmos. Environ.* **35**, 4639–4650 (2001).
50. Decesari, S. *et al.* Enhanced toxicity of aerosol in fog conditions in the Po Valley Italy. *Atmos. Chem. Phys.* **17**, 7721–7731 (2017).
51. Misra, C., Singh, M., Shen, S., Sioutas, C. & Hall, P. M. Development and evaluation of a personal cascade impactor sampler (PCIS). *J. Aerosol Sci.* **33**, 1027–1047 (2002).
52. Singh, M., Misra, C. & Sioutas, C. Field evaluation of a personal cascade impactor sampler (PCIS). *Atmos. Environ.* **37**, 4781–4793 (2003).
53. Chow, J. C. *et al.* The IMPROVE\_A temperature protocol for thermal/optical carbon analysis: Maintaining consistency with a long-term database. *J. Air Waste Manag. Assoc.* **57**, 1014–1023 (2007).
54. Schauer, J. J., Kleeman, M. J., Cass, G. R. & Simoneit, B. R. T. Measurement of emissions from air pollution sources. 2. C1 through C30 organic compounds from medium duty diesel trucks. *Environ. Sci. Technol.* **33**, 1578–1587 (1999).
55. Herner, J. D., Green, P. G. & Kleeman, M. J. Measuring the trace elemental composition of size-resolved airborne particles. *Environ. Sci. Technol.* **40**, 1925–1933 (2006).
56. Lough, G. C. *et al.* Emissions of metals associated with motor vehicle roadways. *Environ. Sci. Technol.* **39**, 826–836 (2005).
57. Turpin, B. J. & Lim, H.-J. Species contributions to PM<sub>2.5</sub> mass concentrations: Revisiting common assumptions for estimating organic mass. *Aerosol Sci. Technol.* **35**, 602–610 (2001).
58. Weber, S. *et al.* Source apportionment of atmospheric PM10 oxidative potential: Synthesis of 15 year-round urban datasets in France. *Atmos. Chem. Phys.* **21**, 11353–11378 (2021).
59. Visentin, M., Pagnoni, A., Sarti, E. & Pietrogrande, M. C. Urban PM<sub>2.5</sub> oxidative potential: Importance of chemical species and comparison of two spectrophotometric cell-free assays. *Environ. Pollut.* **219**, 72–79 (2016).
60. Kurihara, K. *et al.* Contribution of physical and chemical properties to dithiothreitol-measured oxidative potentials of atmospheric aerosol particles at urban and rural sites in Japan. *Atmosphere (Basel)* **13**, 319 (2022).
61. Verma, V. *et al.* Physicochemical and oxidative characteristics of semi-volatile components of quasi-ultrafine particles in an urban atmosphere. *Atmos. Environ.* **45**, 1025–1033 (2011).
62. Cho, A. K., Sioutas, C., Miguel, A. H., Kumagai, Y. & Froines, J. R. Redox activity of airborne particulate matter (PM) at different sites in the Los Angeles Basin. *Environ. Res.* **99**, 40–47 (2005).
63. Verma, V. *et al.* Organic aerosols associated with the generation of reactive oxygen species (ROS) by water-soluble PM<sub>2.5</sub>. *Environ. Sci. Technol.* **49**, 4646–4656 (2015).
64. Verma, V. *et al.* Redox activity of urban quasi-ultrafine particles from primary and secondary sources. *Atmos. Environ.* **43**, 6360–6368 (2009).
65. Charrier, J. G. & Anastasio, C. On dithiothreitol (DTT) as a measure of oxidative potential for ambient particles: Evidence for the importance of soluble newline transition metals. *Atmos. Chem. Phys.* **12**, 9321–9333 (2012).
66. Kumagai, Y. *et al.* Oxidation of proximal protein sulfhydryls by phenanthraquinone, a component of diesel exhaust particles. *Chem. Res. Toxicol.* **15**, 483–489 (2002).
67. Pietrogrande, M. C., Colombi, C., Cuccia, E., Dal Santo, U. & Romanato, L. The impact of COVID-19 lockdown strategies on oxidative properties of ambient PM10 in the Metropolitan Area of Milan Italy. *Environments - MDPI* **9**, 145 (2022).
68. Grezzi, G., Ayuso, R. A., De Vivo, B., Lima, A. & Albanese, S. Lead isotopes in soils and groundwaters as tracers of the impact of human activities on the surface environment: The Domizio-Flegreo Littoral (Italy) case study. *J. Geochem. Explor.* **109**, 51–58 (2011).
69. Chung, J. Y., Yu, S. D. & Hong, Y. S. Environmental source of arsenic exposure. *J. Prevent. Med. Public Health* **47**(5), 253 (2014).
70. Hagemstein, K. The environmental management of selenium in aluminum processing. *JOM* **55**, 51–54 (2003).
71. Harrison, R. M., Jones, A. M., Gietl, J., Yin, J. & Green, D. C. Estimation of the contributions of brake dust, tire wear, and resuspension to nonexhaust traffic particles derived from atmospheric measurements. *Environ. Sci. Technol.* **46**, 6523–6529 (2012).
72. Taghvaei, S. *et al.* Source apportionment of ambient PM<sub>2.5</sub> in two locations in central Tehran using the Positive Matrix Factorization (PMF) model. *Sci. Total Environ.* **628–629**, 672–686 (2018).
73. Tian, W. H. The effect of free adult preventive care services on subsequent utilization of inpatient services in Taiwan. *Int. J. Health Serv.* **46**, 547–565 (2016).
74. Mousavi, A., Sowlat, M. H. & Sioutas, C. Diurnal and seasonal trends and source apportionment of redox-active metals in Los Angeles using a novel online metal monitor and Positive Matrix Factorization (PMF). *Atmos. Environ.* **174**, 15–24 (2018).
75. Yu, J. *et al.* Potassium: A tracer for biomass burning in Beijing?. *Aerosol Air Qual. Res.* **18**, 2447–2459 (2018).
76. Fraser, M. P. & Lakshmanan, K. Using Levoglucosan as a molecular marker for the long-range transport of biomass combustion aerosols. *Environ. Sci. Technol.* **34**, 4560–4564 (2000).

77. Alves, C. A. *et al.* Elements and polycyclic aromatic hydrocarbons in exhaust particles emitted by light-duty vehicles. *Environ. Sci. Pollut. Res.* **22**, 11526–11542 (2015).
78. Karavalakis, G., Boutsika, V., Stournas, S. & Bakeas, E. Biodiesel emissions profile in modern diesel vehicles. Part 2: Effect of biodiesel origin on carbonyl, PAH, nitro-PAH and oxy-PAH emissions. *Sci. Total Environ.* **409**, 738–747 (2011).
79. Masclat, P., Cachier, H., Lioussé, C. & Wortham, H. Emissions of Polycyclic aromatic hydrocarbons by savanna fires. *J. Atmos. Chem.* **22**, 41–54 (1995).
80. Gilardoni, S. *et al.* Fog scavenging of organic and inorganic aerosol in the Po valley. *Atmos. Chem. Phys.* **14**, 6967–6981 (2014).
81. Perrino, C. *et al.* Seasonal variations in the chemical composition of particulate matter: A case study in the Po Valley. Part I: Macro-components and mass closure. *Environ. Sci. Pollut. Res.* **21**, 3999–4009 (2014).
82. Altuwayjiri, A. *et al.* The impact of stay-home policies during Coronavirus-19 pandemic on the chemical and toxicological characteristics of ambient PM<sub>2.5</sub> in the metropolitan area of Milan Italy. *Sci. Total Environ.* **758**, 143582 (2021).
83. Liu, D. *et al.* Concentration, source identification, and exposure risk assessment of PM<sub>2.5</sub>-bound parent PAHs and nitro-PAHs in atmosphere from typical Chinese cities. *Sci Rep* **7**, 10398 (2017).
84. Krůmal, K., Mikuška, P. & Večeřa, Z. Polycyclic aromatic hydrocarbons and hopanes in PM1 aerosols in urban areas. *Atmos. Environ.* **67**, 27–37 (2013).
85. Pepe, N. *et al.* Enhanced CAMx source apportionment analysis at an urban receptor in Milan based on source categories and emission regions. *Atmos. Environ. X* **2**, 100020 (2019).
86. Afzal, A., Cioffi, N., Sabbatini, L. & Torsi, L. NO<sub>x</sub> sensors based on semiconducting metal oxide nanostructures: Progress and perspectives. *Sens. Actuators B Chem.* **171–172**, 25–42 (2012).
87. Whaley, C. H., Galarneau, E., Makar, P. A., Moran, M. D. & Zhang, J. How much does traffic contribute to benzene and polycyclic aromatic hydrocarbon air pollution? Results from a high-resolution North American air quality model centred on Toronto Canada. *Atmos. Chem. Phys.* **20**, 2911–2925 (2020).
88. Longhin, E. M., Mantecca, P. & Gualtieri, M. Fifteen years of airborne particulates in vitro toxicology in milano: Lessons and perspectives learned. *Int. J. Mol. Sci.* **21**, 2489 (2020).
89. Pietrogrande, M. C., Russo, M. & Zagatti, E. Review of PM oxidative potential measured with acellular assays in urban and rural sites across Italy. *Atmosphere (Basel)* **10**, 626 (2019).
90. Perrone, M. G. *et al.* Seasonal variations in chemical composition and in vitro biological effects of fine PM from Milan. *Chemosphere* **78**, 1368–1377 (2010).
91. Simonetti, G., Conte, E., Perrino, C. & Canepari, S. Oxidative potential of size-segregated PM in an urban and an industrial area of Italy. *Atmos. Environ.* **187**, 292–300 (2018).
92. Urch, B. *et al.* Acute blood pressure responses in healthy adults during controlled air pollution exposures. *Environ. Health Perspect.* **113**, 1052 (2005).
93. Delfino, R. J. *et al.* Air pollution exposures and circulating biomarkers of effect in a susceptible population: Clues to potential causal component mixtures and mechanisms. *Environ. Health Perspect.* **117**, 1232–1238 (2009).
94. Delfino, R. J. *et al.* Traffic-related air pollution and blood pressure in elderly subjects with coronary artery disease. *Epidemiology* **21**, 396–404 (2010).
95. Kim, S. Y. *et al.* The temporal lag structure of short-term associations of fine particulate matter chemical constituents and cardiovascular and respiratory hospitalizations. *Environ. Health Perspect.* **120**, 1094 (2012).
96. Delfino, R. J. *et al.* Associations of primary and secondary organic aerosols with airway and systemic inflammation in an elderly panel cohort. *Epidemiology* **21**, 892–902 (2010).

## Acknowledgements

This study was financially supported by the National Institute of Health (Grant Number: 2R01AI065617-22). The authors are also grateful to the Viterbi School of Engineering, University of Southern California (USC) Ph.D. fellowship award.

## Author contributions

Y.A. contributed to the conceptualization, methodology, formal analysis, data curation, visualization, and writing - original draft. M.B. contributed to the conceptualization, methodology, formal analysis, data curation, and writing - review & editing. R.T. contributed to the methodology, data curation, and writing - review & editing. G.S. contributed to the methodology and data curation. R.B. contributed to the data curation and writing - review & editing. A.B. contributed to the data curation and writing - review & editing. C.D. contributed to the data curation and writing - review & editing. P.C. contributed to the data curation and writing - review & editing. A.R. contributed to the methodology, data curation, resources, and writing - review & editing. V.V. contributed to the methodology, data curation, and writing - review & editing. T.C. contributed to the funding acquisition, resources, and writing - review & editing. C.S. contributed to the conceptualization, project administration, funding acquisition, supervision, resources, and writing - review & editing.

## Competing interests

The authors declare no competing interests.

## Additional information

**Supplementary Information** The online version contains supplementary material available at <https://doi.org/10.1038/s41598-024-55292-2>.

**Correspondence** and requests for materials should be addressed to C.S.

**Reprints and permissions information** is available at [www.nature.com/reprints](http://www.nature.com/reprints).

**Publisher's note** Springer Nature remains neutral with regard to jurisdictional claims in published maps and institutional affiliations.



**Open Access** This article is licensed under a Creative Commons Attribution 4.0 International License, which permits use, sharing, adaptation, distribution and reproduction in any medium or format, as long as you give appropriate credit to the original author(s) and the source, provide a link to the Creative Commons licence, and indicate if changes were made. The images or other third party material in this article are included in the article's Creative Commons licence, unless indicated otherwise in a credit line to the material. If material is not included in the article's Creative Commons licence and your intended use is not permitted by statutory regulation or exceeds the permitted use, you will need to obtain permission directly from the copyright holder. To view a copy of this licence, visit <http://creativecommons.org/licenses/by/4.0/>.

© The Author(s) 2024